Prosthetic Legs Output Feedback Control via Variable High Gain Observer

Alessandro J. Peixoto, Ignácio de A. M. Ricart and Matheus Ferreira dos Reis

Abstract—This paper address the state estimation and control of a robot/prosthesis control system with four joints: vertical hip displacement, thigh, knee and ankle angles. The motivation was inspired by several drawbacks regarding the usage of load cells and/or sensors in robots and prosthetic legs to capture gait data, external forces (GRFs) and moments during walking. We propose the implementation of a high gain observer (HGO) to estimate the prosthesis joint velocities with a time varying HGO gain synthesized from measurable signals designed to reduce the amount of noise in the control effort while keeping an acceptable tracking error transient performance. Numerical simulations analyze the robustness of the closed loop control with respect to parametric errors and measurement noise.

I. INTRODUCTION

Prosthesis are devices that substitute the function of a missing limb either due to amputation or a congenital defect. Amputations could occur due to injuries, circulatory and vascular disease, diabetes or cancer and that means a huge number of people that could maintain their activities of daily livings (ADLs) and have the mobility partially / completely restored through improvements in prosthesis technology.

There are three main types of prosthesis currently available: purely passive, active-damping controlled and powered controlled prostheses [1]. The first type requires a significant effort from the amputee because there are only passive mechanical systems to assist him during the gait. Active damping uses microprocessors and sensors to measure when knee flexion and extension is needed based on encoder measures and load transfer acquired from observer/load cells. In this way, it can actively regulate the prosthesis damping factor and help the user during stance phases and during the gait.

A powered controlled prosthesis requires less metabolic energy from the user for walking than purely passive because they are able to generate net power at the joints through DC electrical motors or pneumatic actuators [2] [3]. As they are able to supply positive power, the user could more easily realize tasks such as climbing stairs and walking uphill.

The sensors usually used in this type of prosthesis measure the joint angles with high-resolution encoders and contact forces via strain gauges or load cells. Angular velocities could be acquired through expensive tacometers or can be estimated via numerical differentiation. In general, numerical approaches for velocity estimations are implemented via observers or filtered estimates like "dirty" derivatives. However, noise attenuation is a well known challenge is those cases. State estimation via Extended Kalman Filter (EKF), High-gain-observer (HGO) and Sliding Mode Observer (SMO) are promising as well as the estimation of forces acting on the prosthetic foot.

In contrast to [4], where an Extended Kalman Filter is designed to estimate joint position, velocities and ground reaction forces, here an HGO based estimation approach is deployed. Time-varying HGOs have also been used to cope with the effect of measurement noise and to establish the connections with the Extended Kalman Filter [5] [6].

Output-feedback control strategies using HGOs [7] represent an important design class, in particular, the schemes based on time-varying high gain techniques (HGO with variable gain) [8] [9] [10] [11] [5]. In [12], [13], an output-feedback sliding-mode control design have been proposed for arbitrary relative degree uncertain systems, where the class of plants encompasses time-varying minimum phase nonlinear plants, affine in the control, transformable to a normal form and for which a norm state estimator can be implemented. The main objective in [12] was to use a dynamic observer gain in order to obtain global results without invoking the global Lipschitz-like restrictions.

In the present paper, considering that robot/prosthesis system has parametric uncertainties and angle measurement is subject to noise, a time-varying HGO design is proposed, similar to [12]. This variable gain approach is different from most of the existing techniques, where the HGO gain is updated either solving a Riccati equation [8] [14] [15] or via functions based on measurable signals and norm domination techniques [11], [14], [16] and [12]. While estimating in real-time the noise energy presented in the control effort, an adaptation law changes the observer gain to achieve a acepptable trade-off between control signal noise and tracking performance. Global results are not pursued in this paper. A proportional-integral-derivative (PID) conventional control with feedback linearization is developed in order to make a robotic prosthetic leg follow a desired walking pattern. The proposed approach is verified in a simulation environment with a 4-link robot/prosthesis system (PRRR), with parameters extracted from [17]. The human gait used as reference signal is obtained from [18].

II. PRELIMINARIES

The following notations and terminology are used:
- The 2-norm (Euclidean) of a vector x and the corresponding induced norm of a matrix A are denoted by $|x|$ and $|A|$, respectively. The symbol $\lambda[A]$ denotes the spectrum of A and $\lambda_m[A] = -\max_i\{Re\{\lambda[A]\}\}$.
- The $\mathscr{L}_{\infty e}$ norm of a signal $x(t) \in \mathbb{R}^n$ is defined as $\|x_t\| := \sup_{0 \le \tau \le t} |x(\tau)|$.
- The symbol "s" represents either the Laplace variable or the differential operator "d/dt", according to the context.
- As in [19] the output y of a linear time invariant (LTI) system with transfer function $H(s)$ and input u is given by

$y = H(s)u$. Convolution operations $h(t) * u(t)$, with $h(t)$ being the impulse response from $H(s)$, will be eventually written, for simplicity, as $H(s) * u$.

- Classes of $\mathcal{K}, \mathcal{K}_\infty$ functions are defined according to [20, p. 144]. ISS, OSS and IOSS mean Input-State-Stable (or Stability), Output-State-Stable (or Stability) and Input-Output-State-Stable, respectively [21].
- The symbol π denotes class-$\mathcal{KL}$ functions. Eventually, we denote by $\pi(t)$ any exponentially decreasing signal, i.e., a signal satisfying $|\pi(t)| \leq \Pi(t)$, where $\Pi(t) := Re^{-\lambda t}$, $\forall t$, for some scalars $R, \lambda > 0$.

III. System Model

The dynamics of the machine/prosthesis system composed by a 4-link rigid body robot[1] with prismatic-revolute-revolute-revolute (PRRR) configuration, following the notation in [17], is given by:

$$D(q)\ddot{q} + C(q,\dot{q})\dot{q} + B(q,\dot{q}) + P(\dot{q}) + J_e^T F_e + g(q) = F_a, \quad (1)$$

where q represents the vector of joints positions (q_1 represents the hip vertical displacement, q_2 is the thigh angle, q_3 is the knee angle and q_4 represents ankle angle), $D(q)$ is the inertia matrix, $C(q,\dot{q})$ is the matrix of Coriolis and centrifugal forces, $B(q,\dot{q})$ is the knee damper nonlinear matrix, J_e is the kinematic Jacobian relative to the point of application of external forces F_e, $g(q)$ is the term of gravitational forces and F_a is the torque/force produced by the actuators. Here, in contrast to [17], we have included the term $P(\dot{q})$ in order to take explicitly into account the Coulomb friction as in [22]. Note that, inertial and frictional effects in the actuators can be included in this model.

To establish a basis for dynamic model derivations and to verify the leg geometry during simulations, the set of reference frames used for forward kinematics problems are the same as the ones assigned in [17]. Matrices $D(q)\ddot{q}$, $C(q,\dot{q})$ and $g(q)$ are obtained using the standard Newton-Euler/Euler-Lagrange approach with the plant parameters extracted from [17].

A. A Simplified Model

In order to illustrate the observer design proposed in this note, consider a simplified version of the machine/prosthesis system (2) where no external forces are considered ($F_e \equiv 0$), the specific leg prosthesis damping matrix is disregarded ($B(q,\dot{q}) \equiv 0$) and the Coulomb friction is neglected ($P(\dot{q}) \equiv 0$). In this case, the machine/prosthesis system is described by:

$$D(q)\ddot{q} + C(q,\dot{q})\dot{q} + g(q) = F_a. \quad (2)$$

The system matrices $D(q), C(q,\dot{q})$ and $g(q)$ are supposed to be uncertain, but the corresponding nominal matrices $D_n(q), C_n(q,\dot{q})$ and $g_n(q)$ are assumed known. In particular, the inertia matrix $D(q)$ which is invertible, since $D(q) = D^T(q)$ is strictly positive definite.

[1]A more general framework with a n-link rigid body robot can also be considered. However, in order to keep this note close to [17], for simplicity, we have set $n = 4$.

Introducing the variables $x_1 := q \in \mathbb{R}^4$ and $x_2 := \dot{q} \in \mathbb{R}^4$, the model (2) can be rewritten in the state-space form as:

$$\dot{x}_1 = x_2, \quad (3)$$
$$\dot{x}_2 = k_p(x,t)[u + d(x,t)], \quad u := F_a \in \mathbb{R}^{4 \times 1}, \quad (4)$$
$$y = x_1, \quad (5)$$

or, equivalently,

$$\dot{x} = A_\rho x + B_\rho k_p(x,t)[u + d(x,t)], \quad (6)$$
$$y = C_\rho x, \quad (7)$$

where $x^T = \begin{bmatrix} x_1 & x_2 \end{bmatrix}$ is the state vector, $k_p(x,t) = D(x_1)^{-1} \in \mathbb{R}^{4 \times 4}$, $d(x,t) := -C(x_1,x_2)x_2 - g(x_1) \in \mathbb{R}^{4 \times 1}$, $C_\rho = \begin{bmatrix} I_{4 \times 4} & 0_{4 \times 4} \end{bmatrix} \in \mathbb{R}^{4 \times 8}$ and the pair (A_ρ, B_ρ) is in Brunovskys canonical controllable form and is given by:

$$A_\rho = \begin{bmatrix} 0_{4 \times 4} & I_{4 \times 4} \\ 0_{4 \times 4} & 0_{4 \times 4} \end{bmatrix} \in \mathbb{R}^{8 \times 8},$$

and

$$B_\rho = \begin{bmatrix} 0_{4 \times 4} & I_{4 \times 4} \end{bmatrix}^T \in \mathbb{R}^{8 \times 4}.$$

For each solution of (6) there exists a maximal time interval of definition given by $[0, t_M)$, where t_M may be finite or infinite. Thus, finite-time escape is not precluded, *a priori*.

Remark. (**Nominal Values**) Nominal terms can be used in the HGO implementation in order to reduce conservatism in the HGO design. The plant could be rewritten as:

$$\dot{x}_1 = x_2, \quad (8)$$
$$\dot{x}_2 = f(x_1,x_2,u,t) + \delta_f(x_1,x_2,u,t), \quad u := F_a, \quad (9)$$
$$y = x_1, \quad (10)$$

where the nominal part of the system dynamics is represented by

$$f(x_1,x_2,u,t) := D_n^{-1}(x_1)u - D_n^{-1}(x_1)\left[C_n(x_1,x_2)x_2 + g_n(x_1)\right], \quad (11)$$

while the uncertainties are concentrated in the term

$$\begin{aligned} \delta_f(x_1,x_2,u,t) := & \left[D^{-1}(x_1) - D_n^{-1}(x_1)\right]u + \\ & \left[D_n^{-1}(x_1)C_n(x_1,x_2) - D^{-1}(x_1)C(x_1,x_2)\right]x_2 + \\ & \left[D_n^{-1}(x_1)g_n(x_1) - D^{-1}(x_1)g(x_1)\right]. \end{aligned} \quad (12)$$

However, to simplify this presentation while keeping the main HGO design methodology, consider $C_n \equiv 0$, $g_n \equiv 0$ and, since D is assumed known, we also have $D_n = D$.

IV. High Gain Observer with Variable Gain

The HGO [23] is given by

$$\dot{\hat{x}} = A_\rho \hat{x} + B_\rho k_p^n u + H_\mu L_o(y - C_\rho \hat{x}), \quad (13)$$

where k_p^n is a nominal value of the plant high frequency gain (HFG) k_p and L_o and H_μ are given by:

$$L_o = \begin{bmatrix} l_1 I_{4 \times 4} & l_2 I_{4 \times 4} \end{bmatrix}^T \in \mathbb{R}^{8 \times 4} \quad (14a)$$
$$H_\mu := \text{diag}(\mu^{-1} I_{4 \times 4}, \ \mu^{-2} I_{4 \times 4}) \in \mathbb{R}^{8 \times 8}. \quad (14b)$$

The observer gain L_o is such that $s^2 + l_1 s + l_2$ is Hurwitz. In this paper, instead of using a constant μ, we introduce a *variable* parameter $\mu = \mu_{(t)} \neq 0, \forall t \in [0, t_M)$, of the form

$$\mu(\omega, t) := \frac{\bar{\mu}}{1 + \psi_\mu(\omega, t)}, \qquad (15)$$

where ψ_μ, named **adapting function**, is a non-negative function continuous in its arguments and ω is an available signal, both to be designed later on. The parameter $\bar{\mu} > 0$ is a design constant. For each system trajectory, μ is absolutely continuous and $\mu \leq \bar{\mu}$. Note that μ is bounded for t in any finite sub-interval of $[0, t_M)$. Therefore,

$$\mu(\omega, t) \in [\underline{\mu}, \bar{\mu}], \quad \forall t \in [t_*, t_M), \qquad (16)$$

for some $t_* \in [0, t_M)$ and $\underline{\mu} \in (0, \bar{\mu})$.

A. High Gain Observer Error Dynamics

The transformation [7]

$$\zeta := T_\mu \tilde{x}, \quad T_\mu := [\mu^2 H_\mu]^{-1} \in \mathbb{R}^{8 \times 8}, \quad \tilde{x} := x - \hat{x}, \qquad (17)$$

is fundamental to represent the $\tilde{x}$-dynamics in convenient coordinates allowing us to show that $\tilde{x}$ is arbitrarily small, *modulo* exponentially decaying term. First, note that:

$$(i) \; T_\mu(A_\rho - H_\mu L_o C_\rho) T_\mu^{-1} = \frac{1}{\mu} A_o, \quad (ii) \; T_\mu B_\rho = B_\rho,$$

$$\text{and} \quad (iii) \; \dot{T}_\mu T_\mu^{-1} = \frac{\dot{\mu}}{\mu} \Delta,$$

where $A_o := A_\rho - L_o C_\rho$ and $\Delta := \mathrm{diag}(-I_{4 \times 4}, \; 0_{4 \times 4}) \in \mathbb{R}^{8 \times 8}$. Then, subtracting (13) from (6) and applying the above relationships (i), (ii) and (iii), the dynamics of $\tilde{x}$ in the new coordinates ζ (17) is given by:

$$\mu \dot{\zeta} = [A_o + \dot{\mu}(t) \Delta] \zeta + B_\rho [\mu \nu], \qquad (18)$$

where

$$\nu := (k_p - k_p^n) u + k_p d, \qquad (19)$$

and

$$\dot{\mu}(t) = -\frac{\mu^2}{\bar{\mu}} \left[\frac{\partial \psi_\mu}{\partial \omega} \dot{\omega} + \frac{\partial \psi_\mu}{\partial t} \right]. \qquad (20)$$

The HGO gain $(H_\mu L_o)$ is inversely proportional to the small parameter μ, allowed to be time-varying. Our task is to establish properties for the adapting function $\psi_\mu(\omega, t)$ in (15) so that $\mu|\nu|$ and $|\dot{\mu}|$ are arbitrarily small, at least after a finite time interval. In fact, we design ψ_μ so that the following inequalities hold

$$|\dot{\mu}(t)|, \; \mu|\nu| \leq \mathcal{O}(\bar{\mu}), \quad \forall t \in [t_\mu, t_M). \qquad (21)$$

for some finite $t_\mu \in [0, t_M)$. Consequently, $\dot{\mu}$ does not *ultimately* affect the stability of A_o in (18) and ζ can be made arbitrarily small, *modulo* an exponentially decaying term, by applying a time scale changing in (18). In addition, since $\tilde{x} = T_\mu^{-1} \zeta$ and $\|T_\mu^{-1}\|$ is of order $\mathcal{O}(1)$, then one can conclude that $\tilde{x}$ can also be made arbitrarily small, *modulo* an exponentially decaying term.

It is clear that inequalities in (21) depend on the choice of the control signal u in (19), the disturbance and the signal ω.

B. The Adapting Function ψ_μ

The adapting function $\psi_\mu(\omega, t)$ used in the time-varying parameter

$$\mu(\omega, t) := \frac{\bar{\mu}}{1 + \psi_\mu(\omega, t)}, \qquad (22)$$

defined in (15), can assume different forms depending on the choice of the signal ω and the available information about the plant.

As an example, consider the following cases:

1) **From a theoretical point of view**: the adapting function ψ_μ can be chosen in order to allow global/semi-global stability (or only convergence) properties for the closed-loop control system.

   a) **Norm Observability**: The plant (6)–(7) admits a norm observer which provides an upper bound for the plant state norm by using only available signals: plant input (u) and plant output (y). In this case, global or semi-global results could be obtained when, for example, a sliding mode based control is employed, as in [12]. More precisely, a norm observer for system (6)–(7) is a m-order dynamic system of the form:

$$\tau_1 \dot{\omega}_1 = -\omega_1 + u, \qquad (23)$$
$$\tau_2 \dot{\omega}_2 = \gamma_o(\omega_2) + \tau_2 \varphi_o(\omega_1, y, t), \qquad (24)$$

   with states $\omega_1 \in \mathbb{R}$, $\omega_2 \in \mathbb{R}^{m-1}$ and positive constants τ_1, τ_2 such that for $t \in [0, t_M)$: (i) if $|\varphi_o|$ is uniformly bounded by a constant $c_o > 0$, then $|\omega_2|$ can escape at most exponentially and there exists $\tau_2^*(c_o)$ such that the ω_2-dynamics is BIBS (Bounded-Input-Bounded-State) stable w.r.t. φ_o for $\tau_2 \leq \tau_2^*$; (ii) for each $x(0), \omega_1(0), \omega_2(0)$, there exists $\bar{\varphi}_o$ such that

$$|x(t)| \leq \bar{\varphi}_o(\omega(t), t) + \pi_o(t), \quad \omega := [\omega_1 \; \omega_2^T \; y]^T, \quad (25)$$

   where $\pi_o := \beta_o(|\omega_1(0)| + |\omega_2(0)| + |x(0)|) e^{-\lambda_o t}$ with some $\beta_o \in \mathcal{K}_\infty$ and positive constant λ_o.

   b) **Global Stability Properties**: when the class of plants are such that a norm observer can be implemented, then **global** results can be achieved via OFSM control, as in [12]. This is the case when, for example, the Coriolis term can be neglected ($C(x_1, x_2) x_2 \equiv 0$).

   c) **Semi-Global Stability Properties**: the nonlinearities appearing in the input disturbance term $d(x, t)$ can always be norm bounded afinelly in the state norm, i.e., there are positive constants M and N such that

$$\|d(x, t)\| \leq M\|x\| + N,$$

   where M, N depends on the plant/controller initial conditions. This dependence is a directly consequence of the smoothness assumption usually considered regarding the nonlinear terms in the robot dynamic equation. Indeed, by assuming that $\|x(0)\| < R_0$, there exist constants $R > 0$ and $t_R > 0$ such that $\|x(t)\| < R$, for $t < t_R$. Therefore, the nonlinear term $d(x, t)$ satisfies $\|d(x, t)\| \leq M\|x\| + N$ for some constants M, N depending on R (or R_0). Then **semi-global** results can be achieved via a particular case of the OFSM control

given in [12]. This is the case when, for example, the Coriolis term can not be neglected ($C(x_1, x_2)x_2 \neq 0$).

2) **From a practical point of view**: the adapting function ψ_μ can be chosen in order to allow local stability (or only convergence) properties for the closed-loop control system. Moreover, one can select a time-varying adapting function ψ_μ to assure an acceptable level of noise in the control signal while keeping a good transient for the output tracking error.

   a) **The system states can be assumed bounded**: The plant state, in particular the unavailable state x_2, is uniformly bounded. Such assumption of the state boundedness is true, for example, when (6) is BIBS stable, and the control input is bounded. Moreover, by considering that the acceleration ($\dot{x}_2$) in the mechanical system is bounded by a known constant, then a constant upper bound for the velocity x_2 can be found by using the "dirty derivative":

$$\eta := \frac{s}{\tau s + 1} y. \tag{26}$$

   Indeed, by noting that

$$x_2 = \eta + \frac{\tau}{\tau s + 1} \dot{x}_2, \tag{27}$$

   one can obtain the following norm bound

$$|x_2| \leq |\eta| + \mathcal{O}(\tau)|\dot{x}_2|. \tag{28}$$

   In this case, we can use this rough estimate for $\dot{x}_2$ and less conservative estimates for the terms depending on y, so that ω can be implemented.

   b) **Signal-to-Noise Ratio in** $|u| \times$ **Tracking Error Norm**: By using some measurement of the amount of noise in the control signal, for example, the Signal-to-Noise Ratio (SNR), the adapting function can be implemented as a function of the SNR and the tracking error, so that μ increases when the SNR in the control effort increases and μ decreases when the tracking error norm increases. This can be accomplished, for example, by defining a cost function depending on the control signal-to-noise ratio and the output tracking error, so that the time-varying μ reaches an optimum value.

C. One Particular Design for ψ_μ

When the plant (6)–(7) admits a norm observer with ω defined in (25) such that

$$|x(t)| \leq \bar{\varphi}_o(\omega(t), t) + \pi_o(t), \tag{29}$$

then norm bounds for the signals $\nu, \dot{\omega}$ and $\dot{\mu}$ can be obtained so that [12]:

$$|\dot{\mu}(t)|, \ \mu|\nu| \leq \mathcal{O}(\bar{\mu}), \quad \forall t \in [t_\mu, t_M), \tag{30}$$

where $t_\mu \in [0, t_M)$. In this case, using the OFSM control described in [12], global, semi-global or local stability and/or convergence properties can be assured by noting that the output tracking error dynamics (and the full error system dynamics) is ISS w.r.t. HGO estimate error which can be made

of order $\mathcal{O}(\bar{\mu})$ after the small finite time instant t_μ. For more details, see [12].

In this paper, we are focused in the following particular choice for time varying HGO gain $\mu(t)$ where noise energy in the control signal and tracking error are taken into account:

$$\mu(\omega, t) := \frac{\alpha \mathcal{N}\{u\}}{1 + \beta|e|} = \frac{\bar{\mu}}{1 + \psi_\mu(\omega, t)}, \tag{31}$$

where α, β are positive design constants, $\mathcal{N}\{u\} > 0$ is the noise energy in the control effort, which can be extracted from several methodologies such as the Signal-to-Noise ratio of the control signal $u(t)$, and e is the tracking error. Note that, this choice fits the general format (15) with $\psi_\mu(\omega, t) = [(1 + \beta|e|)\bar{\mu} - \alpha \mathcal{N}\{u\}]/(\alpha \mathcal{N}\{u\})$ and $\bar{\mu}$ small enough to assure that $\psi_\mu(\omega, t) > 0$.

V. PROBLEM FORMULATION AND CONTROL SCHEMES STABILITY PROPERTIES

The *control objective* is to reduce the tracking error

$$e(t) := y_d - y, \tag{32}$$

where the desired trajectory y_d is ideally a set of joint angles acquired for human gait analysis [18]. For simplicity a second-order model reference linear filterhas been designed so that the reference signal is actually a filtered version of human gait desired angles. This allows us to obtain directly the time-varying derivatives $\dot{y}_d$ and $\ddot{y}_d$ from the state vector representation of the model reference filter.

A PID controller with feedforward is employed just to validate the time-varying HGO proposed in this note. By recalling that we consider $D_n(y) = D(y)$ to simplify the paper presentation, the control signal is given by

$$u(t) := D(y)u_v + C_n(y, \hat{x}_2)\hat{x}_2 + g_n(y), \tag{33}$$

$$u_v(t) := \ddot{q}_d + K_p e(t) + \underbrace{K_d(\dot{y}_d - \hat{x}_2)}_{\approx K_d \frac{de(t)}{dt}} + K_i \int_{t_o}^{t} e\, dt, \tag{34}$$

where $\hat{x}_2$ is the estimate for x_2 obtained from the HGO. The gains are designed in order to match the following equations

$$s^3 + K_d s^2 + K_p s + K_i = 0, \tag{35}$$

$$(s^2 + 2\zeta\omega_n + \omega_n^2)(s + p) = 0, \tag{36}$$

where ω_n, ζ and p are design constants and $K_i := k_i(I_{4 \times 4})$, $K_p := k_p(I_{4 \times 4})$ and $K_d := k_d(I_{4 \times 4})$. Therefore the controller gains are designed in order to approximate the error third order dynamics to a second order system added to a (fast) pole. To this end, the control gains are designed as:

$$k_i := \omega_n^2 p, \tag{37}$$

$$k_p := \omega_n^2 + 2\zeta\omega_n p, \tag{38}$$

$$k_d := p + 2\zeta\omega_n. \tag{39}$$

Note that, in the ideal case when the nominal matrices C_n and g_n match the real values and $\hat{x}_2 = x_2$, the following closed-loop equation holds

$$\dddot{e} + K_d \ddot{e} + K_p \dot{e} + K_i e = 0, \tag{40}$$

μ	x_1 (m)	x_2 (rad)	x_3 (rad)	x_4 (rad)	$\dot{x}_1$ (m/s)	$\dot{x}_2$ (rad/s)	$\dot{x}_3$ (rad/s)	$\dot{x}_4$ (rad/s)
0.4e-3	0.0004	0.0002	0.0009	0.0004	0.0159	0.0117	0.0959	0.0492
1.9e-3	0.0035	0.0013	0.0033	0.0062	0.1120	0.0587	0.2405	0.6836
Variable	0.0008	0.0004	0.0025	0.0059	0.0257	0.0375	0.2268	0.6640

which assures that $|e(t)| \to 0$ as $t \to \infty$ when $s^3 + K_d s^2 + K_p s + K_i = 0$ has strictly stable roots. However, when uncertainties in the plant parameters and/or errors in the HGO estimate are presented, the tracking error converges (locally) to some residual set. On the other hand, when the OFSM control scheme given in [12] is considered, global/semi-global stability results can be guaranteed. The formal proof of this stability results were omitted to save space and to focus on the HGO variable gain behaviour. However, we highlight that the OFSM control scheme developed in [12] can be directly applied here. This was left for a future work.

VI. NUMERICAL SIMULATIONS

The plant initial conditions are: $y(0) = x_1(0) = \begin{bmatrix} 0.0216 & 0.5675 & -0.13 & -0.39 \end{bmatrix}^T$ and $x_2(0) = \begin{bmatrix} 0 & 0 & 0 & 0 \end{bmatrix}^T$. The PID control gains were obtained by considering $\omega_n = 16\pi$, $\zeta = 0.9$, $p = 2\omega_n$. The time varying HGO gain was implemented as in (31) with $\alpha = 10^{-5}$ and $\beta = 1$.

In the present case, it is considered a random parametric error in plant parameters from [17] such as center of gravity, inertia matrix, link length. But the values won't differ by more than 10% from the real value. A white gaussian noise has also been added to the systems output, representing a disturbance needed to be compensated. That will help to illustrate an HGO variable gain application.

The HGO with static gain is implemented with $l_1 = 2$, $l_2 = 6$ and $\mu = \bar{\mu} = 0.001$.

In Fig. 1, Fig. 2, Fig. 3 and Fig. 4 it can be noticed that each joint has its own trajectory and initial condition, which affect differently the estimated state overshoot before convergence. However, every joint estimation converges at approximately 7 ms and the highest overshoot happens in the thigh angle because of its initial condition error (0.57π).

Due to parametric errors and high frequency dynamics, the highest tracking error happens on the ankle angle, which takes more than 100ms to converge. Another interesting tracking error behavior occurs at hip displacement while changing orientation with all the system inertia, causing a higher tracking error than in any other moment and also making the control signal to even saturate in order to follow the trajectory.

The corresponding hip, thigh, knee and ankle velocities are illustrated in Fig. 5, Fig. 6, Fig. 7 and Fig. 8, respectively. The RMSE for tracking error in Table. I shows that velocities in knee and ankle joints require a faster control law to track. That happens because of higher frequency components which also contribute to a worst state estimation in HGO.

A variable HGO gain ($\mu_{var}(t)$) dynamic is depicted in Fig.9, converging to approximately 0.001 in $t = 4s$, while there are two other values shown. In blue, a static $\mu_1 = 4e - 4$ and, in
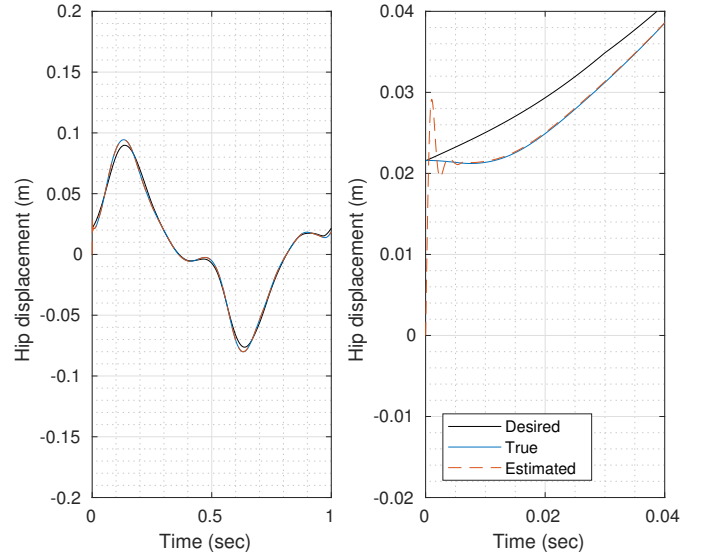

Fig. 1. Simulation results from a desired hip movement, the controlled plant state and the estimated state from the HGO with constant parameter $\mu = 0.001$. The right plot shows the signals behaviors until the first 40ms of simulation
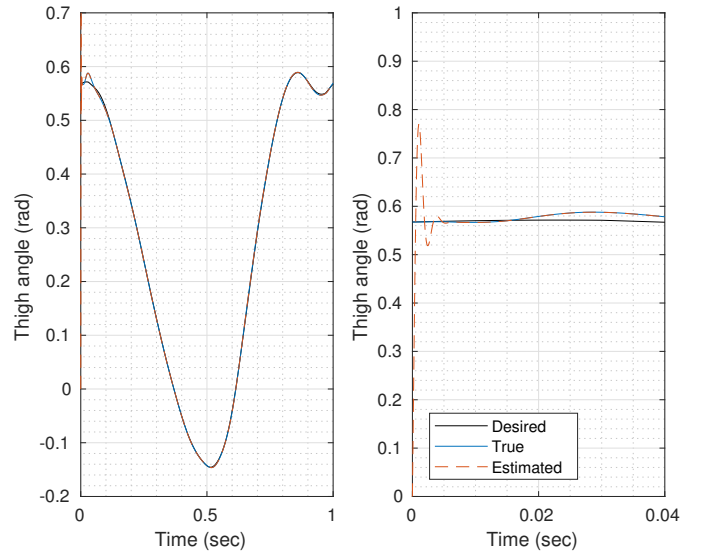

Fig. 2. Simulation results from a desired thigh movement, the controlled plant state and the estimated state from the HGO with constant parameter $\mu = 0.001$. The right plot shows the signals behaviors until the first 40ms of simulation

yellow, the static $\mu_2 = 19e - 4$. In Figs.11 and 10 the same legend pattern in applied as in Fig.9, therefore blue, yellow and red represent μ_1, μ_2 and $\mu_{var}(t)$ respectively.

By applying μ_2, an apparent degradation in the closed-loop tracking error transient is shown in Table I and 12. On the other hand, the noise amplitude in the control signal is acceptable as can be observed in Fig.10 with the corresponding measurement of the noise amplitude illustrated in Fig.11. The noise amplitude was obtained by filtering the control input u with a high-pass filter.

By reducing μ to the constant small value $\mu_{var}(t) = 0.0004$, the tracking error transient is improved in exchange of an increase on the control signal noise, see Fig.11, 12 and Table I.
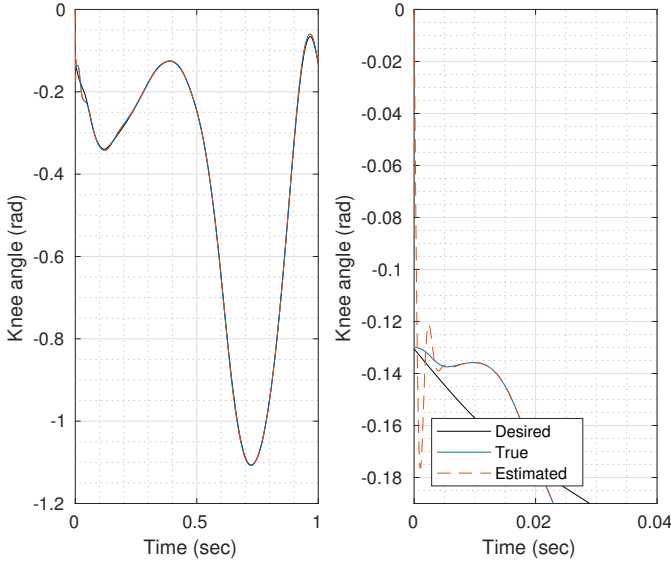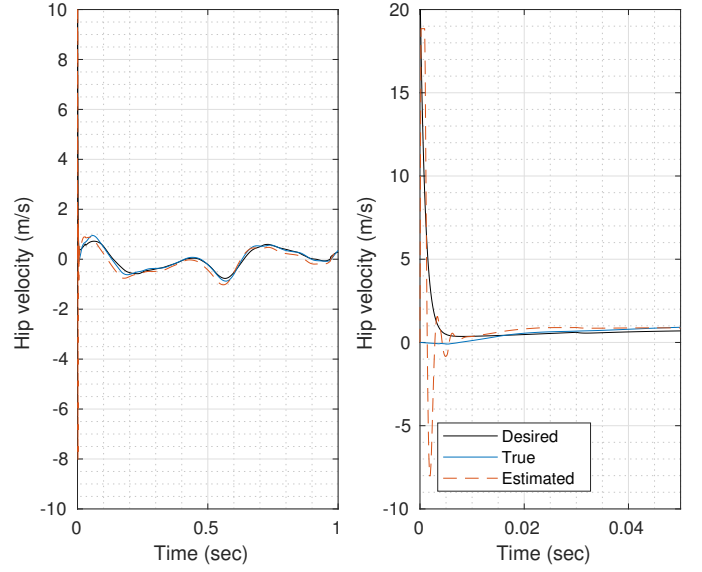
Fig. 3. Simulation results from a desired knee movement, the controlled plant state and the estimated state from the HGO with constant parameter $\mu = 0.001$. The right plot shows the signals behaviors until the first 40ms of simulation
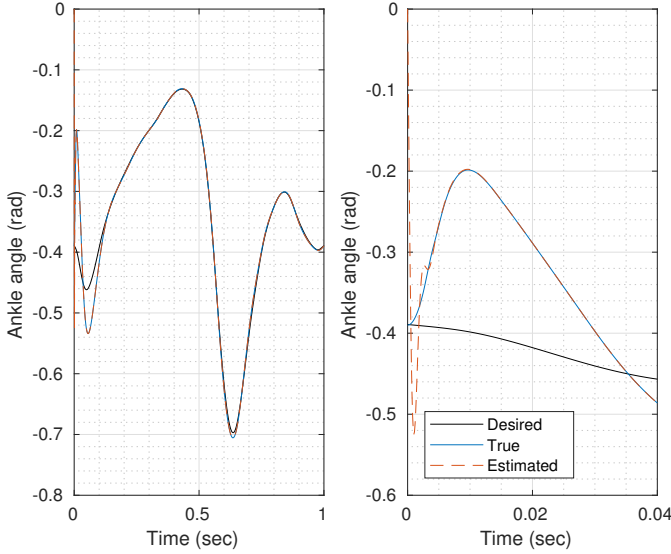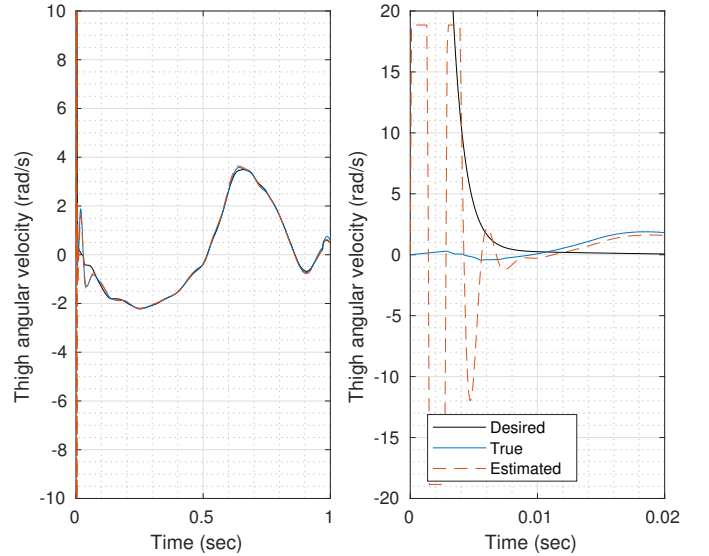

Fig. 5. Simulation results from a desired hip velocity, the controlled plant state and the estimated state from the HGO with constant parameter $\mu = 0.001$. The right plot shows the signals behaviors until the first 15ms of simulation.

Fig. 4. Simulation results from a desired ankle movement, the controlled plant state and the estimated state from the HGO with constant parameter $\mu = 0.001$. The right plot shows the signals behaviors until the first 40ms of simulation

Fig. 6. Simulation results from a desired thigh velocity, the controlled plant state and the estimated state from the HGO with constant parameter $\mu = 0.001$. The right plot shows the signals behaviors until the first 15ms of simulation.

VII. Conclusions and Future Work

In this paper we considered the state estimation problem of a robot/prosthesis control system with vertical hip displacement, thigh, knee and ankle joints. It was verified that it is possible to apply HGO with dynamic gain in order to reduce the

On the other hand, when the time-varying $\mu_{var}(t)$ is implemented starting with the same large value for $\mu_{var}(0) = 0.0019$, the tracking error transient is improved without reducing μ to a prohibitive value which can cause a large noise in the control signal.

The time evolution of $\mu_{var}(t)$ is shown in Fig.9, from which one can verify that μ reaches a value of $\mu_{var}(t) = 0.001$ depending on the noise power applied to the system. This value is not known *a priori*. It is clear that care must be taken while reducing $\bar{\mu}$, since there exists a trade off between noise reduction and tracking accuracy.

TABLE II
ESTIMATION ROOT-MEAN-SQUARE-ERROR (RMSE) OF A HUMAN GAIT FOR EACH JOINT OF A PROSTHETIC LEG WITH ESTIMATED STATES ACCORDING TO THE OBSERVER GAIN μ

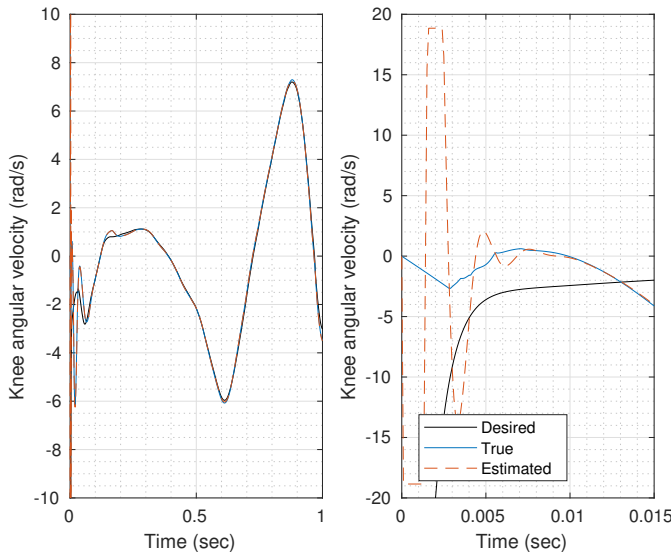| μ	x_1 (m)	x_2 (rad)	x_3 (rad)	x_4 (rad)	$\dot{x}_1$ (m/s)	$\dot{x}_2$ (rad/s)	$\dot{x}_3$ (rad/s)	$\dot{x}_4$ (rad/s)
0.4e-3	0.0001	0.0036	0.0008	0.0024	0.2607	0.4228	0.3570	0.4065
1.9e-3	0.0004	0.0065	0.0015	0.0045	0.3973	0.7754	0.5952	0.8514
Variable	0.0003	0.0065	0.0015	0.0045	0.3167	0.7724	0.5948	0.8512

Fig. 7. Simulation results from a desired knee velocity, the controlled plant state and the estimated state from the HGO with constant parameter $\mu = 0.001$. The right plot shows the signals behaviors until the first 15ms of simulation.
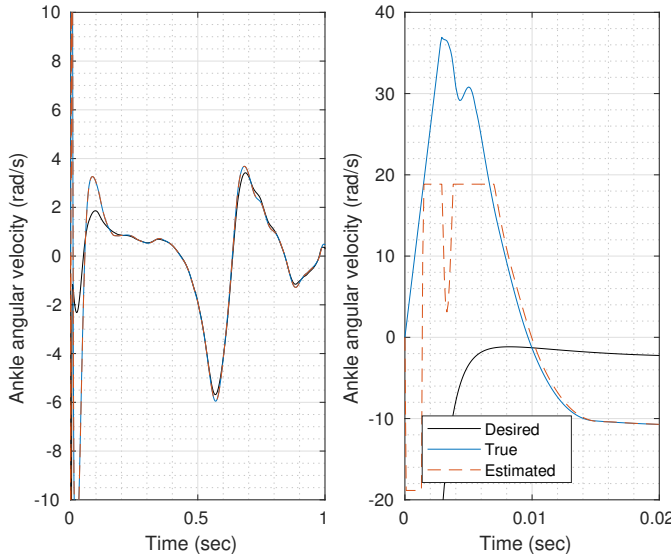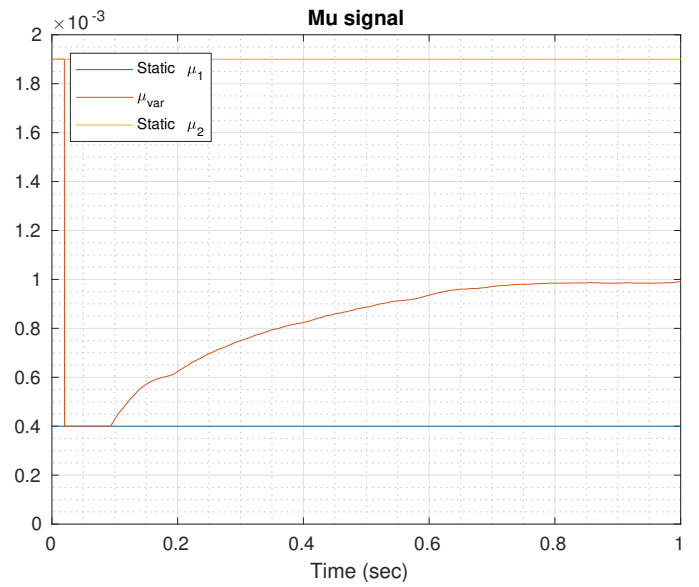

Fig. 9. Simulation results showing the dynamics from variable and static μ.

Fig. 8. Simulation results from a desired ankle velocity, the controlled plant state and the estimated state from the HGO with constant parameter $\mu = 0.001$. The right plot shows the signals behaviors until the first 15ms of simulation.
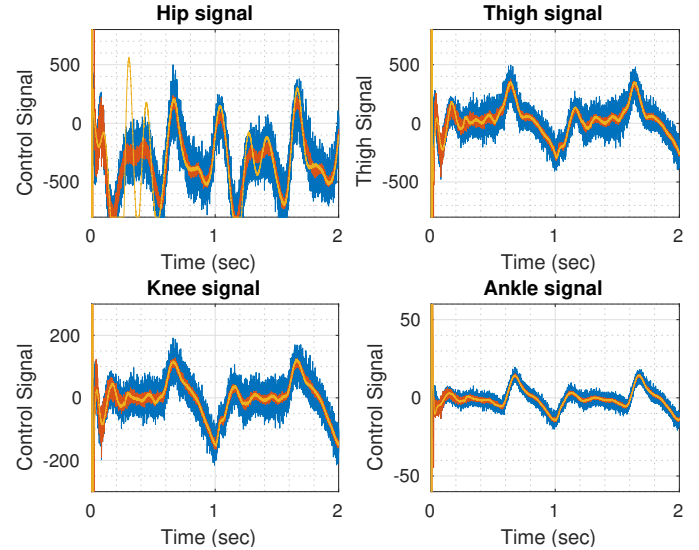

Fig. 10. This graphic shows the difference between gain values and its filtering capacity. The control signal in blue represents the static gain $\mu = 0.0004$, which does not filter the noise as much as $\mu_{var}(t)$ in red or $\mu = 0.0019$ in yellow.

amount of noise in the control signal while assuring an reasonable output tracking error transient. Moreover, when a norm observer is available, domination techniques can be used to design the HGO dynamic gain to obtain global/semi-global practical tracking, via sliding mode control. An illustrative academic simulation example was presented.

Future possible topics of research are: (i) consider the full robot/prosthesis model including the ground reaction forces estimation; (ii) replace the conventional PID controller by a smooth version of the output feedback sliding mode controller previous developed in [12] in order to increase the robustness of the closed loop system w.r.t. parameter uncertainties while assuring global/semi-global stability properties and (iii) perform experimental results.

References

[1] M. I. A. et al., "Towards a smart semi-active prosthetic leg: Preliminary assessment and testing," *Internation Federation of Automatic Control*, vol. 49, no. 21, pp. 170–76, 2016.

[2] G. M. Sup F, Bohara A, "Design and control of a powered transfemoral prosthesis," *The International journal of robotics research*, vol. 27, no. 2, pp. 263–73, 2008.

[3] B. S, "Actuated leg prosthesis for above knee amputees," Patent US7 314 490B2, 2002.

[4] S. A. Fakoorian and D. Simon, "Ground reaction force estimation in prosthetic legs with an extended kalman filter," *Systems Conference (SysCon), 2016 Annual IEEE*, pp. 1–6, 2016.

[5] J. H. Ahrens and H. K. Khalil, "Closed-loop behavior of a class of nonlinear systems under EKF-based control," *IEEE Trans. Aut. Contr.*, vol. 52, no. 3, pp. 536–540, 2007.

[6] ——, "High-gain observers in the presence of measurement noise: A switched-gain approach," *Automatica*, vol. doi:10.1016/j.automatica.2008.11.012, 2009.
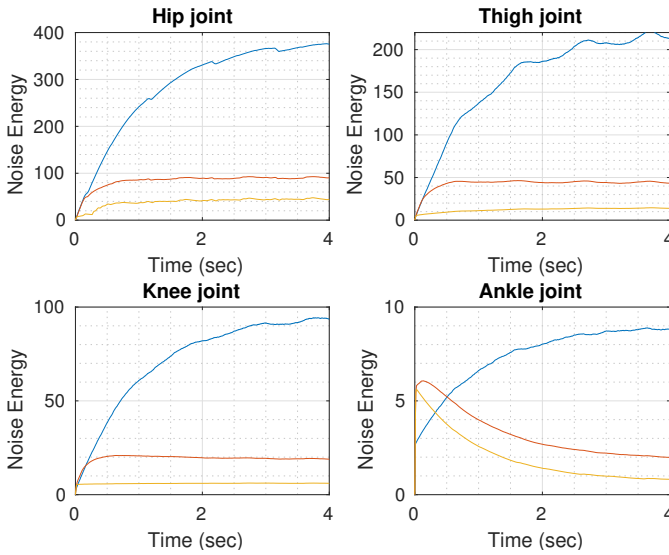
Fig. 11. $\mu_{var}(t)$ in red is able to filter noise as good as $\mu = 0.0019$ in yellow.
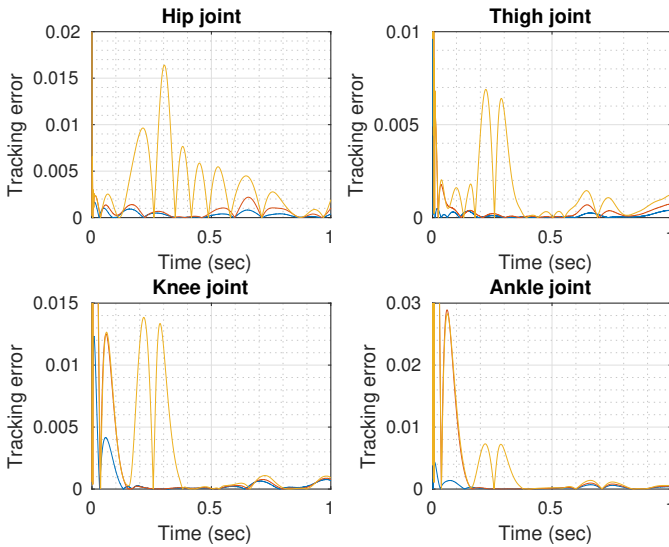

Fig. 12. Using $\mu_{var}(t)$, in red, the system is able to track the trajectory as good as when $\mu = 0.0004$ in blue. For quantitative values, Table I shows tracking RMSE.

[7] S. Oh and H. K. Khalil, "Nonlinear output-feedback tracking using high-gain observer and variable structure control," *Automatica*, vol. 33, no. 10, pp. 1845–1856, 1997.

[8] L. Praly, "Asymptotic stabilization via output feedback for lower triangular systems with output dependent incremental rate," in *Proc. IEEE Conf. on Decision and Control*, Orlando, Florida USA, 2001, pp. 3808–3813.

[9] P. Krishnamurthy, F. Khorrami, and Z. P. Jiang, "Global output feedback tracking for nonlinear systems in generalized output-feedback canonical form," *IEEE Trans. Aut. Contr.*, vol. 47, no. 5, pp. 814–819, 2002.

[10] P. Krishnamurthy, F. Khorrami, and R. S. Chandra, "Global high-gain-based observer and backstepping controller for generalized output-feedback canonical form," *IEEE Trans. Aut. Contr.*, vol. 48, no. 12, pp. 2277–2284, 2003.

[11] H. Lei and W. Lin, "Universal output feedback control of nonlinear systems with unknown growth rate," in *Preprints of the 16th IFAC World Congress*, Prague, Czech Republic, July 2005.

[12] A. J. Peixoto, T. R. Oliveira, and L. Hsu, "Global tracking sliding mode control for a class of nonlinear systems via variable gain observer," *International Journal of Robust and Nonlinear Control*, pp. 177–196, 2011.

[13] A. J. Peixoto, L. Hsu, R. R. Costa, and F. Lizarralde, "Global tracking sliding mode control for uncertain nonlinear systems based on variable high gain observer," in *Proc. IEEE Conf. on Decision and Control*, New Orleans, LA, USA, 2007, pp. 2041–2046.

[14] V. Andrieu, L. Praly, and A. Astolfi, "Asymptotic tracking of a state trajectory by output-feedback for a class of non linear systems," in *CDC*, New Orleans, LA, USA, 2007, pp. 5228–5233.

[15] G. Kaliora, A. Astolfi, and L. Praly, "Norm estimators and global output feedback stabilization of nonlinear systems with ISS inverse dynamics," *IEEE Trans. Aut. Contr.*, vol. 51, no. 3, pp. 493–498, 2006.

[16] V. Andrieu, L. Praly, and A. Astolfi, "High gain observers with updated gain and homogeneous correction terms," *Automatica*, vol. 45, no. 2, pp. 422–428, 2009.

[17] H. Richter, D. Simon, W. A. Smith, and S. Samorezov, "Dynamic modeling, parameter estimation and control of a leg prosthesis test robot," *Applied Mathematical Modelling*, vol. 39, no. 2, pp. 559–573, 2015.

[18] M. H. Schwartz, A. Rozumalski, and J. P. Trost, "The effect of walking speed on the gait of typically developing children," *Journal of Biomechanics*, vol. 41, no. 8, pp. 1639 – 1650, 2008. [Online]. Available: http://www.sciencedirect.com/science/article/pii/S0021929008001450

[19] P. Ioannou and J. Sun, *Robust Adaptive Control*. Prentice-Hall, 1996.

[20] H. K. Khalil, *Nonlinear Systems*, 3rd ed. Prentice Hall, 2002.

[21] E. D. Sontag and Y. Wang, "On characterizations of the input-to-state stability property," *Systems & Contr. Letters*, vol. 24, pp. 351–359, 1995.

[22] J. Lee, R. Mukherjee, and H. K. Khalil, "Output feedback stabilization of inverted pendulum on a cart in the presence of uncertainties," *Automatica*, vol. 54, pp. 146–157, 2015.

[23] H. K. Khalil, "High-gain observers in nonlinear feedback control," *2008 International Conference on Control, Automation and Systems*, pp. xlvii – lvii, 2008.